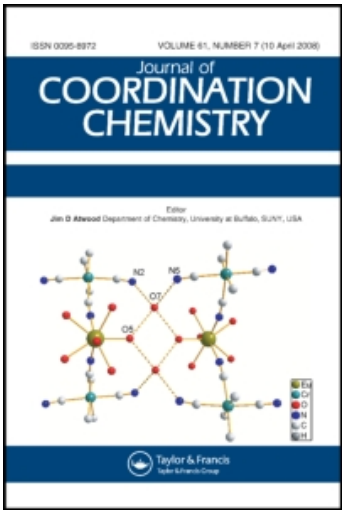

Journal of Coordination Chemistry
Publication details, including instructions for authors and subscription information:
http://www.informaworld.com/smpp/title~content=t713455674

Spectral and thermal studies of alloxan complexes

Moamen S. Refat[a]; Sabry A. EL-Korashy[b]; Deo Nandan Kumar[c]; Ahmed S. Ahmed[a]
[a] Faculty of Education, Department of Chemistry, Port Said, Suez Canal University, Port Said, Egypt [b] Faculty of Science, Department of Chemistry, Ismalia, Suez Canal University, Ismalia, Egypt [c] Department of Chemistry, Deshbandhu College, University of Delhi, Delhi-110019, India

To cite this Article Refat, Moamen S. , EL-Korashy, Sabry A. , Kumar, Deo Nandan and Ahmed, Ahmed S.(2008) 'Spectral and thermal studies of alloxan complexes', Journal of Coordination Chemistry, 61: 12, 1935 — 1950
To link to this Article: DOI: 10.1080/00958970701793636
URL: http://dx.doi.org/10.1080/00958970701793636

Journal of Coordination Chemistry
Vol. 61, No. 12, 20 June 2008, 1935–1950

Taylor & Francis
Taylor & Francis Group

Spectral and thermal studies of alloxan complexes

MOAMEN S. REFAT*†, SABRY A. EL-KORASHY‡,
DEO NANDAN KUMAR§ and AHMED S. AHMED†

†Faculty of Education, Department of Chemistry, Port Said, Suez Canal University,
Mohamed Ali Street, Port Said, Egypt
‡Faculty of Science, Department of Chemistry,
Ismalia, Suez Canal University, Ismalia, Egypt
§Department of Chemistry, Deshbandhu College, University of Delhi,
Delhi-110019, India

(*Received 21 June 2007; in final form 18 August 2007*)

The complexes of alloxan with Cr(III), Mn(II), Fe(III), Co(II), Ni(II), Cu(II), Zn(II) Cd(II), Hg(II), Ti(IV) and Zr(II) have been isolated and characterized on the basis of elemental analysis, molar conductivity, spectral studies (mid infrared, ^{1}H-NMR and UV/vis spectra), X-ray powder diffraction (XRD) and scanning electron microscopy (SEM). The thermal decomposition of the metal complexes was studied by thermogravimetric analysis (TGA) and differential thermal analysis (DTA). The kinetic thermodynamic parameters, E^*, ΔH^*, ΔS^* and ΔG^*, were calculated using Coats and Redfern and Horowitz and Metzger equations. The ligand and its complexes have been studied for possible biological activity including antibacterial and antifungal activity.

Keywords: Alloxan; Infrared spectra; Thermal studies; Thermodynamic parameters; Microbiological screening

1. Introduction

Pyrimidine derivatives are known for their varied biological properties. Brugnatelli [1] was the first to isolate ''Alloxan'', a pyrimidine derivative, in 1818 and later this compound was found to possess antineoplastic properties [2].

Alloxan (2,4,5,6 [1H,3H]-pyrimidinetetrone), (H_2L), is widely used in studies of diabetes because this agent destroys pancreatic islet β-cells with a specific selectivity [3–5]. A study on the mechanism of action of the typical diabetogenic agent is of great importance for elucidating the cause of insulin-dependent diabetes mellitus. Alloxan inhibits proinsulin synthesis in pancreatic islets [6]. Uchigata *et al*. proposed that alloxan caused DNA strand breaks to stimulate nuclear poly(ADP-ribose) synthetase, thereby depleting intracellular NAD level and inhibiting proinsulin synthesis [7, 8]. Actually, islet DNA strand breaks were observed *in vivo* by administration of alloxan to rats [9].

Also, alloxan is capable of influencing calcium, zinc, and phosphorus metabolism in organisms by increasing the blood sugar. Therefore, it can be used in experimental studies of diabetes [10]. Moreover, alloxan occurs in living organisms, and is the product of uric

*Corresponding author. Email: msrefat@yahoo.com

Journal of Coordination Chemistry
ISSN 0095-8972 print/ISSN 1029-0389 online © 2008 Taylor & Francis
DOI: 10.1080/00958970701793636

acid decomposition [11]. High biological activity of alloxan imparts interest in its complexation reactions. Thus, Co(II), Ni(II), and Cu(II) complexes with alloxan, $ML_2 \cdots 5H_2O$, were isolated from aqueous alkaline solutions [12]; manganese(II) alloxanate was obtained by evaporation of an acidified solvent at room temperature [13]. From spectrophotometric data, cerium(III) forms a soluble complex ML_2 with alloxan [14]. Transition-metal salts react with alloxan solutions to give colored complexes: orange-yellow or red for Cd(II), Mg(II), Cu(II), Zn(II), Co(II), Ni(II), dark blue (in the presence of ammonia) for Fe(II) [15]. The compositions and properties of Pb(II), Hg(I), Hg(II), and Ag(I) alloxanates were not studied in detail [15–18]. Previously, Kovalchukova *et al.* [19, 20] studied Fe(III) and Co(III) complexes with alloxan; the syntheses of Co(II), Ni(II), and Pd(II) alloxanates were also reported [21]. Study of complexation of a series of *d* and *f* block metals with alloxan was done by Shebaldina *et al.* [22].

The present investigation is undertaken to study the course of interaction between alloxan and different transition metal ions, Cr(III), Mn(II), Fe(III), Co(II), Ni(II), Cu(II), Zn(II), Cd(II), Hg(II), Ti(IV) and Zr(IV). The solid products were characterized spectroscopically. The stabilities of the alloxanate complexes were checked using thermogravimetric analysis and thermodynamic calculations. The biological screening of these complexes compared with free alloxan was reported against different bacterial and fungi species.

2. Experimental

2.1. *Materials and instrumentation*

All chemicals were reagent grade and used without further purification. Alloxan was purchased from Fluka Chemical Co., $CrCl_3 \cdot 6H_2O$, $MnCl_2 \cdot 4H_2O$, $FeCl_3$, $CoCl_2 \cdot 6H_2O$, $NiCl_2 \cdot 6H_2O$, $CuCl_2 \cdot 2H_2O$, $ZnBr_2$, $CdCl_2$, $HgCl_2$, $TiCl_4$ and $ZrCl_4$ from Merck Co.

Carbon and hydrogen contents were determined using a Perkin-Elmer CHN 2400. The metal content was found gravimetrically by converting the compounds into their corresponding oxides at 800°C under air.

IR spectra were recorded on a Genesis II FTIR spectrometer in the 4000–400 cm^{-1} range with 40 scans in KBr discs. The UV-Vis spectra were determined in DMSO at 1.00×10^{-3} M for alloxan and 10 complexes using a Jenway 6405 spectrophotometer with 1 cm quartz cell in the range 800–200 nm. Molar conductivities of freshly prepared 1.0×10^{-3} M DMSO solutions were measured using a Jenway 4010 conductivity meter.

^{1}H-NMR spectra of the free ligand, Zn(II) and Co(II) complexes were recorded on Bruker Avance 300 MHz equipment using DMSO-d_6 as solvent and TMS as an internal reference. The X-ray powder diffraction patterns (XRD) were obtained on a Rikagu diffractometer using Cu/Kα radiation. The scanning electron microscope (SEM) images were taken on JEOL-840 equipment, with an accelerating voltage of 15 kV. Simultaneous TGA and DTA curves were obtained on a Rigaku 8150 thermoanalyzer under dynamic nitrogen at a heating rate of 5 deg min^{-1}.

2.2. *Synthesis of metal complexes*

2.2.1. $[CrL(OH)(H_2O)] \cdot H_2O$ (1). Alloxan (0.48 g, 3.0 mmol) was dissolved in 25 mL methanol. This solution was added to 10 mL methanolic solution of $CrCl_3 \cdot 6H_2O$

(0.266 g, 1.0 mmol) with continuous stirring for 3 h. The mixture was warmed to ~60°C and sodium hydroxide added to adjust the pH to 8.5. Immediately, deep green precipitate occurred, was collected by filtration, washed several times by minimum amounts of hot methanol and dried under *vacuo* over anhydrous $CaCl_2$.

2.2.2. [Mn(HL)(OH)(H_2O)] (2). A similar procedure as that described for **1** was carried out by mixing alloxan (0.32 g, 2.00 mmol) with $MnCl_2 \cdot 2H_2O$ (0.198 g, 1.0 mmol) with pH adjusted to 6.69.

2.2.3. [Fe(HL)$(OH)_2(H_2O)_2] \cdot 3H_2O$ (3). A brown complex, $[Fe(HL)(OH)_2(H_2O)_2] \cdot 3H_2O$, was prepared during reaction of alloxan (0.48 g, 3 mmol) with $FeCl_3$ (0.162 g, 1.0 mmol) by a method similar to that used for preparation of **1**; the pH was adjusted to 8.20.

2.2.4. [CoL$(H_2O)_2] \cdot 2H_2O$ (4). A methanolic solution of $CoCl_2 \cdot 6H_2O$ (0.257 g, 1.0 mmol) was mixed with alloxan (0.32 g, 2.0 mmol) in methanol. The mixture stayed at room temperature for 1 h with constant stirring and then heated on a water bath at ~60°C for 30 min and the pH adjusted to 8.20. The violet complex was filtered off, washed several times with hot methanol and dried under *vacuo* over anhydrous $CaCl_2$.

2.2.5. [Ni(HL)$(H_2O)_3Cl] \cdot 2H_2O$ (5). The nickel(II) alloxanate complex was prepared by the same method used for preparation of **2** and **4**. The weight of $NiCl_2 \cdot 6H_2O$ was 0.256 g, 1.0 mmol, mixed with alloxan in (1 : 2) molar ratio. The pH was adjusted to 8.00.

2.2.6. [CuL$(H_2O)_2] \cdot 3H_2O$ (6). A green complex was obtained by following essentially the same procedure as for **4**, with 0.152 g (1.0 mmol) $CuCl_2 \cdot 2H_2O$. The pH was adjusted to 6.0.

2.2.7. [ZnL$(H_2O)_2] \cdot 4H_2O$ (7). $[ZnL(H_2O)_2] \cdot 4H_2O$ was prepared by mixing equal volumes (30 mL) of alloxan (0.32 g, 2.0 mmol) with $ZnBr_2$ (0.224 g, 1.0 mmol). The mixture was titrated with NaOH to pH 6.5 and then heated on a water bath at 60°C with constant stirring for 45 min. A yellow solid complex precipitated, was collected, washed several times with hot methanol and then dried *in vacuo* over anhydrous $CaCl_2$.

2.2.8. [Cd$(HL)_2] \cdot 5H_2O$ (8) and [Hg$(HL)_2] \cdot 5H_2O$ (9). Preparation of these two complexes followed mainly the same procedure as preparation of **7**, but the weights of $CdCl_2$ and $HgCl_2$ were 0.201 g (1.0 mmol) and 0.271 g (1.0 mmol), respectively. The pH was adjusted to 7.5.

2.2.9. [Ti$(HL)_2Cl_2] \cdot 10H_2O$ (10) and [Zr$(HL)_2Cl_2] \cdot 8H_2O$ (11). $[Ti(HL)_2Cl_2] \cdot 10H_2O$ and $[Zr(HL)_2Cl_2] \cdot 8H_2O$ were prepared during reaction of alloxan with $TiCl_4$ and $ZrCl_4$, respectively, in (1 : 2) molar ratio (M(IV) : H_2L) by a method similar to that used for the preparation of **2**. These complexes started to settle down after the pH was adjusted to 7.00, collected by filtration, washed several times with hot methanol and then dried in a vacuum desiccator over $CaCl_2$ for about four days.

2.3. *Microbiological screening*

For these investigations the hole well method was applied [23]. The investigated isolates of bacteria were seeded in tubes with nutrient broth (NB). The seeded NB (1 cm^3) was homogenized in the tubes with 9 cm^3 of melted (45°C) nutrient agar. The homogeneous

suspensions were poured into Petri dishes. The holes (diameter 4 mm) were done in the cool medium. After cooling in these holes, 2×10^{-3} dm^3 of the investigated compounds were applied using a micropipette. After incubation for 24 h in a thermostat at 25–27°C, the inhibition (sterile) zone diameters (including disc) were measured and expressed in mm. An inhibition zone diameter over 7 mm indicates that the tested compound is active against the bacteria under investigation.

The antibacterial activities of the investigated compounds were tested against *Escherichia coli*, *Streptococcus pneumonia* and *Bacillus subtilis* as well as some fungi, *Aspergillus flavus*, *Fusarium solani* and *Penicillium verrcosum*. Alloxan and the pure solvent were also tested. The concentration of each solution was 1.0×10^{-3} M. Commercial DMSO was employed to dissolve the tested samples.

3. Results and discussion

Alloxan is an alterdentate ligand offering more than one equivalent coordination site. In an alterdentate ligand there is, principally, always a rearrangement possible in which the metal is transferred from one site to another. This can be either an inter- or intramolecular process. The rearrangement is kinetically controlled by the activation energy and entropy on the reaction path. The free energy difference is zero by definition, if the coordination sites are equivalent [24, 25].

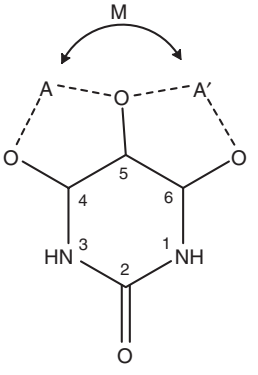

Hydrated alloxan can potentially exist in different tautomeric forms [23, 26]:

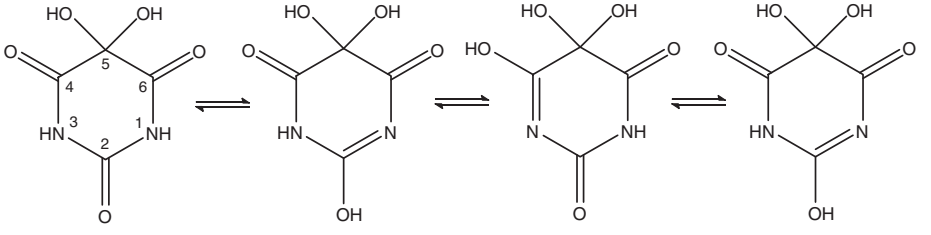

The calculated atomization heats (ΔH) indicated that monoenol II is most stable in the gas phase ($\Delta H = 62.71$ eV). Stabilities of monoenol I, dienol, and lactam forms are somewhat lower ($\Delta H = 62.44$, 62.64, and 62.65 eV, respectively). According to X-ray diffraction data [27, 29], the crystal alloxan molecule exists as the lactam (trioxo) form.

However, close intermolecular interaction energies for above tautomers (4.86, 4.27, 4.53, and 5.22 eV) make it possible that in solutions several forms exist simultaneously and can be stabilized during complexation.

Literature on alloxanate complexes shows that alloxan can coordinate with several types of structures:

Type 1: the metal chelate ring involving oxygen in position 2 and nitrogen in position 1 [23].

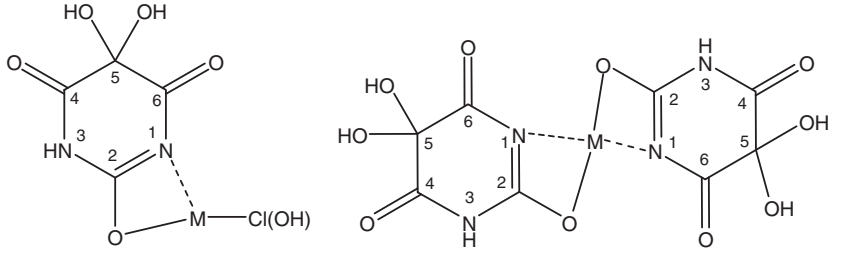

Type 2: the metal chelate ring involving oxygen in position 4 and one of the hydroxyl groups in position 5 [23].

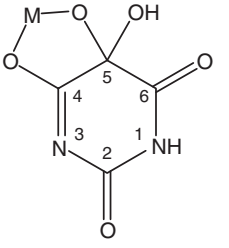

Type 3: the metal chelate ring involving oxygen in position 2 and a hydroxyl in position 5 [23].

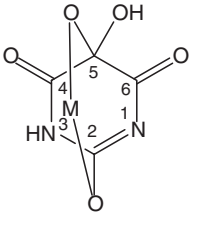

Type 4: the metal chelate ring involving oxygen in position 4 and the nitrogen in position 3 [19, 29].

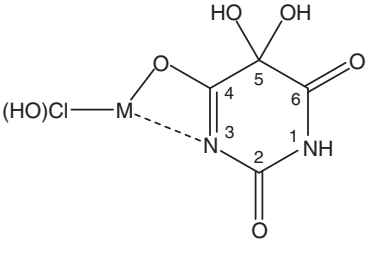

Type 5: the metal chelate ring involving oxygens in positions 4 and 5 [30].

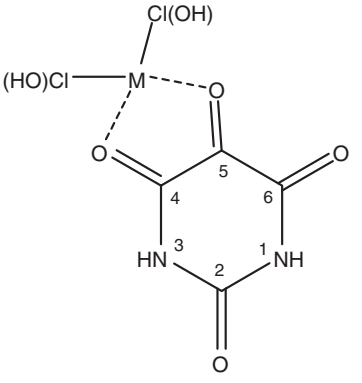

The elemental analyses and some physical characteristics of the compounds are given in table 1.

The complexes are air-stable, hygroscopic, with all melting points over 300°C, insoluble in H_2O and most organic solvents but partially soluble in DMSO.

The elemental analysis data (table 1) of the complexes indicate a 1:1 metal:ligand stoichiometry for $[CrL(OH)(H_2O)]\cdot H_2O$, $[Mn(HL)(OH)(H_2O)]$, $[Fe(HL)(OH)_2(H_2O)_2]\cdot 3H_2O$, $[CoL(H_2O)_2]\cdot 2H_2O$, $[Ni(HL)(H_2O)_3Cl]\cdot 2H_2O$, $[CuL(H_2O)_2]\cdot 3H_2O$ and $[ZnL(H_2O)_2]\cdot 4H_2O$; 1:2 for $[Cd(HL)_2]\cdot 5H_2O$, $[Hg(HL)_2]\cdot 5H_2O$, $[Ti(HL)_2Cl_2]\cdot 10H_2O$ and $[Zr(HL)_2Cl_2]\cdot 8H_2O$.

Table 1. Elemental analyses and physical data of the alloxanate complexes.

Compounds	Mol. wt.	mp (°C)	Color	Content ((calculated) found) % C	% H	% N	% M	Λ_m ($\Omega^{-1}cm^{-1}mol^{-1}$)
$[CrL(OH)(H_2O)]\cdot H_2O$	262.99	>300	Deep green	(18.25)	(2.66)	(10.64)	(19.76)	10.61
(**1**, $C_4H_7N_2O_8Cr$)				18.08	3.20	9.44	19.88	
$[Mn(HL)(OH)(H_2O)]$	248.9	>300	Pale brown	(19.28)	(2.41)	(11.25)	(22.07)	19.77
(**2**, $C_4H_6N_2O_7Mn$)	4			19.03	1.76	11.29	21.95	
$[Fe(HL)(OH)_2(H_2O)_2]\cdot 3H_2O$ (**3**,$C_4H_{15}N_2O_{12}Fe$)	338.85	>300	Brown	(14.17) 14.39	(4.42) 2.43	(8.26) 8.29	(16.48) 16.22	26.60
$[CoL(H_2O)_2]\cdot 2H_2O$	288.93	>300	Violet	(16.61)	(3.46)	(9.69)	(14.84)	15.08
(**4**, $C_4H_{10}N_2O_9Co$)				17.28	3.25	8.91	14.77	
$[Ni(HL)(H_2O)_3Cl]\cdot 2H_2O$	343.20	>300	Green	(13.99)	(3.78)	(8.15)	(17.10)	6.60
(**5**, $C_4H_{13}N_2O_{10}ClNi$)				14.60	3.20	7.35	17.34	
$[CuL(H_2O)_2]\cdot 3H_2O$	311.55	>300	Deep green	(15.40)	(3.85)	(8.98)	(20.39)	28.70
(**6**, $C_4H_{12}N_2O_{10}Cu$)				15.45	2.15	8.29	20.80	
$[ZnL(H_2O)_2]\cdot 4H_2O$	331.38	>300	Yellow	(14.48)	(4.22)	(8.45)	(23.31)	10.27
(**7**, $C_4H_{14}N_2O_{11}Zn$)				14.39	5.45	8.56	23.24	
$[Cd(HL)_2]\cdot 5H_2O$	520.40	>300	Pink	(18.45)	(3.07)	(10.76)	(21.59)	6.90
(**8**, $C_8H_{16}N_4O_{15}Cd$)				18.45	4.25	9.26	21.87	
$[Hg(HL)_2]\cdot 5H_2O$	608.59	>300	Pale violet	(15.77)	(2.62)	(9.20)	(32.95)	38.90
(**9**, $C_8H_{16}N_4O_{15}Hg$)				15.65	5.43	8.45	32.97	
$[Ti(HL)_2Cl_2]\cdot 10H_2O$	616.88	>300	Pale yellow	(15.56)	(4.21)	(9.07)	(7.76)	44.40
(**10**, $C_8H_{26}N_4O_{20}Cl_2Ti$)				16.65	5.43	8.45	7.16	
$[Zr(HL)_2Cl_2]\cdot 8H_2O$	624.22	>300	Pale red	(15.38)	(3.52)	(8.97)	(14.61)	7.07
(**11**, $C_8H_{22}N_4O_{18}Cl_2Zr$)				15.45	6.34	8.89	14.34	

3.1. *Molar conductivities of metal chelates*

The molar conductivity values for alloxanate complexes in DMSO (1.00×10^{-3} mol) were in the range 6.50–44.40 $\Omega^{-1}\,cm^{-1}\,mol^{-1}$, suggesting non-electrolytes (table 1) [31]. The molar conductance values indicate that the anions exist inside the coordination sphere as in $[Ni(HL)(H_2O)_3Cl]\cdot 2H_2O$, $[Ti(HL)_2Cl_2]\cdot 10H_2O$ and $[Zr(HL)_2Cl_2]\cdot 8H_2O$. In the case of Cr(III), Mn(II), Fe(III), Co(II), Cu(II), Zn(II), Cd(II) and Hg(II) alloxan complexes, no chloride ions were present.

3.2. *Infrared spectra*

The main IR data are summarized in table 2 and IR spectra are shown in figure S1 (supplementary data; online only). The IR spectrum of alloxan exhibits an intense band due to the carbonyl with poorly defined maxima at 1764, 1737 and 1726 cm^{-1}. The band at 1764 cm^{-1} was assigned to the alloxan amide fragment (–NH–CO–NH–) and the bands at 1737 cm^{-1} [19, 20] and 1726 cm^{-1} can be attributed to the ketone group in position 5 and the two ketone groups in positions 4 and 6, respectively. In the range 3339–3044 cm^{-1}, broad intense bands due to overlapping NH and OH vibrations were observed.

We can divide alloxanate complexes according to the IR spectra into two groups: Group I: In the spectra of these compounds, $[Mn(HL)(OH)(H_2O)]$, $[Fe(HL)(OH)_2(H_2O)_2]\cdot 3H_2O$, $[Ni(HL)(H_2O)_3Cl]\cdot 2H_2O$, $[Cd(HL)_2]\cdot 5H_2O$, $[Hg(HL)_2]\cdot 5H_2O$, $[Ti(HL)_2Cl_2]\cdot 10H_2O$ and $[Zr(HL)_2Cl_2]\cdot 8H_2O$, the carbonyls in positions 4 and 6 (1727–1711 cm^{-1}) remain unchanged, while the bands at 1764 and 1737 cm^{-1} disappear due to the formation of hydroxyl with the metal chelating the oxygen in position 2 and the nitrogen in position 1 (Type 1). Group 2: In the IR spectra of the other complexes, the three absorption bands of carbonyls disappeared, while absorption intensity in the range 1650–1450 cm^{-1} increases. Metal-chelation involving the carbonyl in position 4 (or 6) can be realized through both pyrimidine nitrogen atom and one hydroxyl in position 5 (Type 2).

The infrared spectra of the $[ZrO]^{2+}$ complex show a medium absorption band at 1073 cm^{-1} due to ν(Zr=O) [32].

Table 2. IR frequencies (cm^{-1}) of alloxan and its metal complexes.

Compound	N(NH) + ν(OH)	ν(C(4)=O), ν(C(6)=O)	ν(N=C–O)
H_2L*	3339–3044	1726	–
1	3352–2854	–	1632
2	3358–2954	1711	1642
3	3350–2920	1722	1614
4	3391–2903	–	1640
5	3381–2834	1723	1624
6	3361–2825	–	1631
7	3391–2817	–	1643
8	3360–2835	1717	1617
9	3350–2850	1727	1614
10	3350–2815	1724	1605
11	3340–2854	1727	1633

*H_2L has ν(C(2)=O) at 1764 cm^{-1} and ν(C(5)=O) at 1737 cm^{-1}.

3.3. *Electronic absorption spectra*

The spectra of the alloxan complexes in DMSO are shown in figure S2 and the spectral data are listed in table 3. There are four absorption bands at 215, 220, 240 and 260 nm, the bands at 215 and 220 nm assigned to π–π^* and the other two assigned to n–π^* intraligand transitions. These transitions are also found in the spectra of the complexes, but shifted, confirming coordination. The second two bands at 240–260 nm are due to presence of ketone groups [21]. The Ni(II), Zn(II), Cd(II), Hg(II), Ti(IV) and Zr(II) complexes have absorption bands at ~400 nm assigned as charge-transfer [33, 34]. The broad band at 615 nm in the spectrum of Co(II) alloxanate complex can be attributed to d–d transition.

3.4. *^{1}H NMR spectra*

The ^{1}H-NMR spectra of alloxan, Co(II) and Zn(II) complexes are shown in figure S3. In the spectrum of the free ligand, there are four peaks, the peaks appearing at 11.23 and 2.25 ppm can be attributed to N–H and O–H in the lactam form. The peak at 7.47 ppm can be attributed to N–H in position 3 when alloxan converted to monoenol I form, confirming the different tautomeric forms of alloxan. The fourth peak at 3.26 ppm is due to the presence of water.

The spectrum of Co(II) complex resembles the Zn(II) complex but both are different from the free ligand. The spectra of the two complexes also contain four peaks. The first peak at 10.25 and 10.05 ppm in the spectra of Co(II) and Zn(II) complexes, respectively, can be attributed to N–H in position 3 (monoenol I form). The second peak at 8.01 and 7.81 ppm can be attributed to N–H in position 1 (monoenol II form) with hydrogen in N–H (position 3) transferred to the nitrogen in position 1 through the carbonyl group in position 2. Those at 3.33 and 3.16 ppm are due to water of hydration. The fourth at 2.49 and 2.33 are attributed to hydroxyl. The presence of these peaks indicate chelating through oxygen in position 4 and a hydroxyl in position 5 (Type 2).

3.5. *X-ray powder diffraction*

X-ray powder diffraction patterns in the $10^\circ < 2\theta < 70^\circ$ of **1–7** were carried out to obtain lattice dynamics. A sample XRD pattern is shown in figure 1. The Cr(II), Mn(II), Cu(II) and Cd(II) complexes are amorphous while Fe(III), Co(II), Ni(II) and Zn(II) complexes are nano-crystalline [35].

3.6. *Scanning electron microscope*

Purity and morphology of the complexes obtained were studied by SEM. The obtained SEM micrographs (sample in figure S4) allow verifying that the complexes are well-formed amorphous shapes, in agreement with the obtained X-ray results. Single crystals of the complexes could not be isolated, thus, no definitive structure can be described.

Table 3. The electronic spectral data of the ligand and complexes.

Compound	λ_{max} (nm)	ε ($mol^{-1}\,cm^{-1}$)	Assignment
H_2L	215	165	π-π^* trans.
	225	205	π–π^* trans.
	240	1061	n–π^* trans.
	260	987	n–π^* trans.
1	215	186	π–π^* trans.
	225	1000	π–π^* trans.
	235	348	n–π^* trans.
	275	813	n–π^* trans.
2	215	194	π–π^* trans.
	230	613	π–π^* trans.
	285	1891	n–π^* trans.
3	215	678	π–π^* trans.
	240	510	n–π^* trans.
	280	1890	n–π^* trans.
4	215	259	π–π^* trans.
	230	127	π–π^* trans.
	240	232	n–π^* trans.
	280	1247	n–π^* trans.
	615	70	d–d trans.
5	220	448	π–π^* trans.
	240	341	n–π^* trans.
	275	318	n–π^* trans.
	400	111	L → Ni C.T.
6	230	2400	π–π^* trans.
	275	2452	n–π^* trans.
	285	2481	n–π^* trans.
7	215	262	π–π^* trans.
	225	323	π–π^* trans.
	235	360	n–π^* trans.
	265	405	n–π^* trans.
	400	112	L → Zn C.T.
8	230	337	π–π^* trans.
	240	837	n–π^* trans.
	275	774	n–π^* trans.
	400	425	L → Cd C.T.
9	215	170	π–π^* trans.
	225	212	π–π^* trans.
	255	723	n–π^* trans.
	285	651	n–π^* trans.
	400	125	L → Hg C.T.
10	225	339	π–π^* trans.
	240	202	n–π^* trans.
	250	339	n–π^* trans.
	275	100	n–π^* trans.
	400	75	L → Ti C.T.
11	210	211	π–π^* trans.
	235	471	π–π^* trans.
	250	260	n–π^* trans.
	285	196	n–π^* trans.
	400	70	L → Zr C.T.

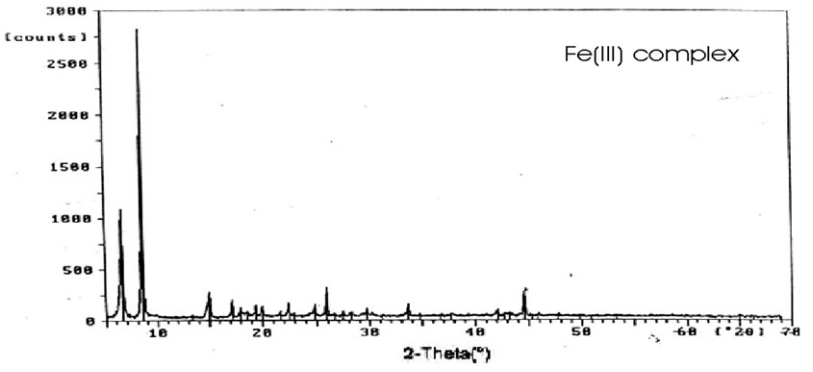

Figure 1. XRD diagrams of Fe(III) alloxanate complex.

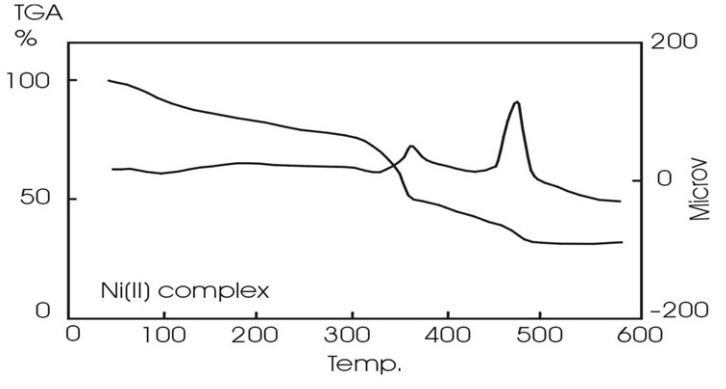

Figure 2. The TG and DTG of the Ni(II) alloxanate complex.

3.7. *Thermogravimetric analysis*

A sample thermal analysis curve (TG and DTG) is shown in figure 2. The thermoanalytical results are summarized in table 4.

The thermal decomposition of alloxan complexes occur at two-to-four steps. The first and second degradation steps of Fe(III), Co(II), Ni(II), Cu(II) and Zn(II) complexes are assigned to release of H_2O molecules inside and outside the coordination sphere. From the second to last decomposition steps deal with loss of alloxan. The final residue in all the complexes was assigned to metal oxides or chlorides.

3.8. *Kinetic studies*

Several equations [36–43] have been proposed as means of analyzing a TG curve and obtaining values for kinetic parameters. Many authors [36–40] have discussed the advantages of this method over the conventional isothermal method. The rate of a decomposition process can be described as the product of two separate functions of temperature and conversion [37], using

$$\frac{d\alpha}{dt} = K(T)f(\alpha) \quad (1)$$

Table 4. Thermal data of the alloxanate complexes.

Compound	Steps	Temperature range (°C)	DTG peak (°C) Endo	DTG peak (°C) Exo	TG Weight loss (%) Calcd	TG Weight loss (%) Found	Assignments
1	1st	50–175	80	–	13.68	13.18	$2H_2O$
	2nd	175–600	375	–	48.29	47.34	$C_2H_3N_2O_{4.5}$ (organic moiety)
					38.02	39.48	$1/2Cr_2O_3 + 2C$ (residue)
2	1st	50–170	120	–	7.23	7.87	H_2O
	2nd	175–600	–	340	53.02	52.40	$C_3H_4N_2O_4$ (organic moiety)
					39.75	39.74	$MnO_2 + C$ (residue)
3	1st	50–150	80	–	15.93	15.76	$3H_2O$
	2nd	150–265	200	–	10.62	10.24	$2H_2O$
	3rd	265–350	–	300	22.14	21.51	$NO_2 + 5/2H_2 + 3/2O_2$
	4th	350–600	–	440	13.58	13.39	NO_2
					37.73	39.10	$1/2Fe_2O_3 + 4C$ (residue)
4	1st	50–150	100	–	12.46	12.86	$2H_2O$
	2nd	150–300	240	–	12.46	12.84	$2H_2O$
	3rd	300–600	–	340	36.68	35.90	$CH_2N_2O_4$ (organic moiety)
					38.39	38.40	$CoO + 3C$ (residue)
5	1st	50–100	75	–	10.49	10.54	$2H_2O$
	2nd	100–300	200	–	15.73	15.46	$3H_2O$
	3rd	300–350	–	330	28.12	28.61	CH_3NO_2Cl (organic moiety)
	4th	350–600	–	420	13.40	13.51	NO_2
					32.26	31.88	$NiO + 3C$ (residue)
6	1st	50–190	100	–	17.33	17.65	$3H_2O$
	2nd	190–220	200	–	11.55	11.35	$2H_2O$
	3rd	220–350	–	300	28.90	28.04	$CH_2N_2O_3$ (organic moiety)
	4th	350–600	–	375	8.99	9.19	CO
					33.23	33.77	$CuO + 2C$ (residue)
7	1st	50–225	120	–	21.72	21.48	$4H_2O$
	2nd	225–300	225	–	10.86	10.59	$2H_2O$
	3rd	300–440	–	410	14.49	14.05	$NO_2 + H_2$
	4th	440–600	–	525	13.88	12.00	NO_2
					39.05	41.88	$ZnO + 4C$ (residue)
8	1st	50–275	175	–	17.20	17.27	$5H_2O$
	2nd	275–600	–	340	39.58	39.95	$4NO_2 + H_2O + 2H_2$
					43.22	42.78	$CdO + 8C$ (residue)
9	1st	50–125	100	–	14.78	14.46	$5H_2O$
	2nd	125–380	–	300	35.17	35.95	$C_6H_6N_4O_5$ (organic moiety)
	3rd	380–600	–	450	14.46	15.30	$2CO_2$
					35.59	34.29	HgO (residue)
10	1st	50–300	150	–	29.18	29.13	$10H_2O$
	2nd	300–600	–	340	37.28	36.07	$C_2H_6N_4O_9$ (organic moiety)
					33.54	34.80	$TiOCl_2 + 6C$ (residue)
11	1st	50–190	120	–	23.07	23.12	$8H_2O$
	2nd	190–320	250	–	24.03	24.29	$C_2H_6N_4O_4$ (organic moiety)
	3rd	320–360	–	340	14.10	14.46	$2CO_2$
	4th	360–600	–	400	4.49	4.58	CO
					34.31	33.55	$ZrOCl_2 + 3C$ (residue)

where α is the fraction decomposed at time t, $k(T)$ is the temperature dependent function and $f(\alpha)$ is the conversion function dependent on the mechanism of decomposition. It has been established that the temperature dependent function $k(T)$ is of the Arrhenius type and can be considered as the rate constant k.

$$k = Ae^{-E^*/RT} \tag{2}$$

where R is the gas constant in ($J\,mol^{-1}\,K^{-1}$). Substituting equation (2) into equation (1), we get

$$\frac{d\alpha}{dT} = \left(\frac{A}{\varphi e^{-E^*/RT}}\right) f(\alpha) \tag{3}$$

where φ is the linear heating rate dT/dt. On integration and approximation, this equation can be obtained in the following form

$$\ln g(\alpha) = \frac{-E^*}{RT} + \ln\left[\frac{AR}{\varphi E^*}\right] \tag{4}$$

where $g(\alpha)$ is a function of α dependent on the mechanism of the reaction. The integral on the right hand side is known as temperature integral and has no closed solution, but several techniques have been used to evaluate the temperature integral. Most commonly used methods for this purpose are the differential method of Freeman and Carroll [36], integral method of Coats and Redfern [38] and the approximation method of Horowitz and Metzger [41].

In the present investigation the general thermal behaviors of the alloxanate complexes in terms of stability ranges, peak temperatures and values of kinetic parameters (sample in figure 3) are given in table 5. The kinetic parameters have been evaluated using the Coats–Redfern equation [44] and the Horowitz–Metzger equation. The results obtained are in agreement with each other.

3.9. *Microbiological investigation*

The results of antibacterial activities *in vitro* of the ligand and the complexes are shown in figure 4 and given in table 6. The complexes have high effect on *Bacillus subtilis* and

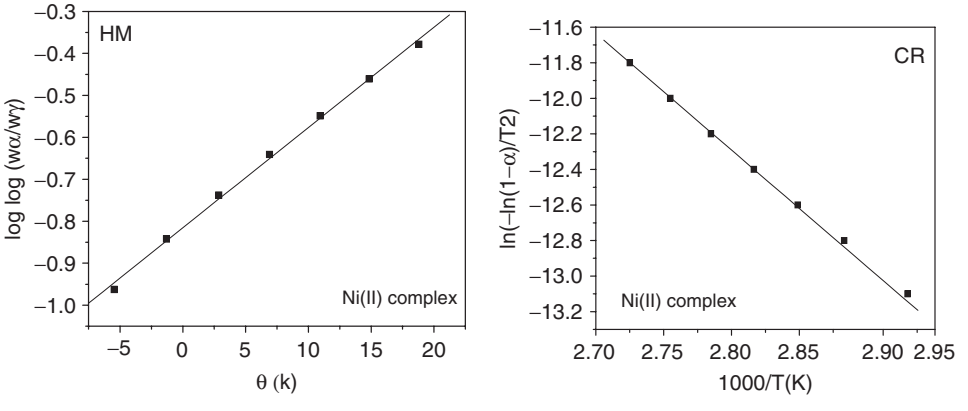

Figure 3. Horowitz–Metzger (HM), Coats–Redfern (CR) of the first step of the Ni(II) alloxanate complex.

Table 5. Kinetic parameters using the Coats–Redfern (CR) and Horowitz–Metzger (HM) operated for the alloxanate complexes.

			Parameter					
Complex	Stage	Method	E (kJ mol^{-1})	A (s^{-1})	ΔS (J mol^{-1} K^{-1})	ΔH (kJ mol^{-1})	ΔG (kJ mol$^{-1)}$	r
1	1st	CR	7.78×10^4	7.21×10^8	−76.7	7.48×10^4	1.02×10^5	0.9885
		HM	7.82×10^4	6.97×10^9	−57.9	7.53×10^4	9.57×10^4	0.9834
		Average	7.80×10^4	3.52×10^9	−67.3	7.50×10^5	9.88×10^4	
	2nd	CR	2.08×10^4	6.19×10^6	-1.21×10^2	1.54×10^4	9.41×10^4	0.9833
		HM	3.31×10^4	1.09×10^6	-2.51×10^2	2.77×10^4	1.90×10^5	0.9992
		Average	2.69×10^4	5.12×10^6	-1.86×10^2	2.15×10^4	1.42×10^5	
2	1st	CR	1.97×10^4	3.66×10^5	-1.41×10^2	1.65×10^4	7.18×10^4	0.9920
		HM	2.71×10^4	2.11×10^4	-2.22×10^2	2.38×10^4	1.11×10^5	0.9999
		Average	2.34×10^4	1.93×10^5	-1.81×10^2	2.01×10^4	9.14×10^5	
	2nd	CR	1.72×10^5	1.51×10^{13}	1.41	1.67×10^5	1.66×10^5	0.9968
		HM	1.97×10^5	1.00×10^{15}	3.63	1.92×10^5	1.70×10^5	0.9959
		Average	1.84×10^5	5.07×10^{14}	2.52	1.79×10^5	1.68×10^5	
3	1st	CR	3.40×10^4	1.87×10^3	-1.84×10^2	3.11×10^4	9.59×10^4	0.9999
		HM	3.94×10^4	6.46×10^3	-1.73×10^2	3.65×10^4	9.77×10^4	0.9912
		Average	3.67×10^4	4.16×10^3	-1.78×10^2	3.38×10^4	9.68×10^4	
	2nd	CR	4.16×10^4	1.33×10^4	-1.70×10^2	3.75×10^4	1.21×10^5	0.9999
		HM	4.17×10^4	1.34×10^2	-2.08×10^2	3.76×10^4	1.40×10^5	0.9990
		Average	4.16×10^4	6.71×10^3	-1.89×10^2	7.75×10^4	1.30×10^5	
4	1st	CR	2.60×10^4	3.41×10^4	-1.60×10^2	2.29×10^4	8.26×10^4	0.9990
		HM	3.15×10^4	1.77×10^2	-2.04×10^2	2.84×10^4	1.04×10^5	0.9993
		Average	2.87×10^4	1.17×10^4	-1.82×10^2	4.89×10^4	9.75×10^5	
	2nd	CR	2.78×10^4	3.18×10^5	-1.44×10^2	2.35×10^4	9.89×10^4	0.9870
		HM	3.67×10^4	1.85×10^2	-2.25×10^2	3.23×10^4	1.50×10^5	0.9980
		Average	8.23×10^4	5.60×10^4	-1.66×10^2	2.56×10^4	1.24×10^5	
5	1st	CR	4.46×10^4	7.28×10^5	-1.34×10^2	5.17×10^4	9.83×10^4	0.9989
		HM	5.55×10^4	2.91×10^6	-1.22×10^2	5.26×10^4	9.52×10^4	0.9987
		Average	5.00×10^4	1.45×10^6	-1.28×10^2	5.21×10^4	9.66×10^4	
	2nd	CR	1.87×10^4	1.32×10^6	-1.32×10^2	1.48×10^4	7.70×10^4	0.9867
		HM	2.51×10^4	1.98×10^2	-2.43×10^2	2.11×10^4	1.36×10^5	0.9974
		Average	2.19×10^4	6.60×10^5	-1.87×10^2	1.79×10^4	1.06×10^5	
6	1st	CR	3.17×10^4	1.89×10^4	-1.65×10^2	2.86×10^4	9.01×10^4	0.9873
		HM	3.97×10^4	3.06×10^3	-1.80×10^2	3.66×10^4	1.04×10^5	0.9878
		Average	3.56×10^4	1.09×10^4	-1.72×10^2	3.26×10^4	9.70×10^4	
	2nd	CR	1.54×10^5	1.25×10^{15}	40.3	1.50×10^5	1.31×10^5	0.9909
		HM	1.61×10^5	1.41×10^{16}	60.4	1.57×10^5	1.29×10^5	0.9864
		Average	1.57×10^4	7.67×10^{15}	50.3	1.53×10^5	1.30×10^5	
7	1st	CR	3.14×10^4	7.07×10^3	-1.73×10^2	2.83×10^4	9.28×10^4	0.9999
		HM	3.77×10^4	1.54×10^3	-1.86×10^2	3.46×10^4	1.04×10^5	0.9990
		Average	3.45×10^4	4.30×10^3	-1.79×10^2	3.14×10^4	9.84×10^4	
	2nd	CR	2.89×10^4	3.31×10^5	-1.44×10^2	2.48×10^4	9.62×10^4	0.9886
		HM	3.65×10^4	2.97×10^2	-2.21×10^2	3.24×10^4	1.42×10^5	0.9999
		Average	3.27×10^4	1.65×10^5	-1.82×10^2	2.86×10^4	1.19×10^5	
8	1st	CR	2.24×10^4	3.97×10^5	-1.41×10^2	1.87×10^4	8.19×10^4	0.9872
		HM	2.93×10^4	1.16×10^4	-2.28×10^2	2.56×10^4	1.28×10^5	0.9906
		Average	2.58×10^4	2.04×10^5	-1.84×10^2	2.21×10^4	1.04×10^5	
	2nd	CR	2.12×10^5	5.33×10^{16}	69.6	2.07×10^5	1.65×10^5	0.9975
		HM	2.08×10^5	3.98×10^{16}	67.2	2.03×10^5	1.64×10^5	0.9975
		Average	2.10×10^5	4.65×10^{16}	68.4	2.05×10^5	1.64×10^5	

(*Continued*)

Table 5. Continued.

Complex	Stage	Method	Parameter					
			E (kJ mol^{-1})	A (s^{-1})	ΔS (J mol^{-1} K^{-1})	ΔH (kJ mol^{-1})	ΔG (kJ mol$^{-1)}$	r
9	1st	CR	5.47×10^4	3.64×10^5	-1.42×10^2	5.16×10^4	1.04×10^5	0.9952
		HM	6.03×10^4	3.57×10^6	-1.21×10^2	5.72×10^4	1.02×10^5	0.9969
		Average	5.75×10^4	1.96×10^6	-1.31×10^2	5.44×10^4	1.03×10^5	
	2nd	CR	4.23×10^4	1.06×10^5	-1.51×10^2	3.92×10^4	9.54×10^4	0.9987
		HM	2.09×10^4	3.81×10^3	-2.36×10^2	1.78×10^4	1.06×10^5	0.9958
		Average	3.16×10^4	5.49×10^4	-1.93×10^2	2.85×10^4	1.00×10^5	
10	1st	CR	3.11×10^4	1.76×10^4	-1.66×10^2	2.80×10^4	8.97×10^4	0.9999
		HM	2.80×10^4	5.11×10^2	-2.14×10^2	2.49×10^4	1.05×10^5	0.9974
		Average	2.95×10^4	9.05×10^3	-2.73×10^2	2.64×10^4	9.73×10^4	
	2nd	CR	1.53×10^5	2.81×10^{11}	-31.5	1.48×10^5	1.67×10^5	0.9907
		HM	1.63×10^5	2.21×10^{12}	-14.4	1.58×10^5	1.55×10^5	0.9985
		Average	1.58×10^4	1.24×10^{12}	-22.9	1.53×10^5	1.61×10^5	
11	1st	CR	3.23×10^4	8.24×10^3	-1.72×10^2	2.92×10^4	9.34×10^4	0.9975
		HM	3.71×10^4	1.23×10^3	-1.88×10^2	3.40×10^4	1.04×10^5	0.9976
		Average	3.47×10^4	4.73×10^3	-1.80×10^2	3.16×10^4	9.87×10^4	
	2nd	CR	1.23×10^5	3.40×10^{11}	-2.80×10^2	1.19×10^5	1.32×10^5	0.9998
		HM	1.22×10^5	5.33×10^{11}	-2.43×10^2	1.18×10^5	1.30×10^5	0.9994
		Average	1.22×10^5	4.36×10^{11}	-2.61×10^2	1.18×10^5	1.31×10^5	

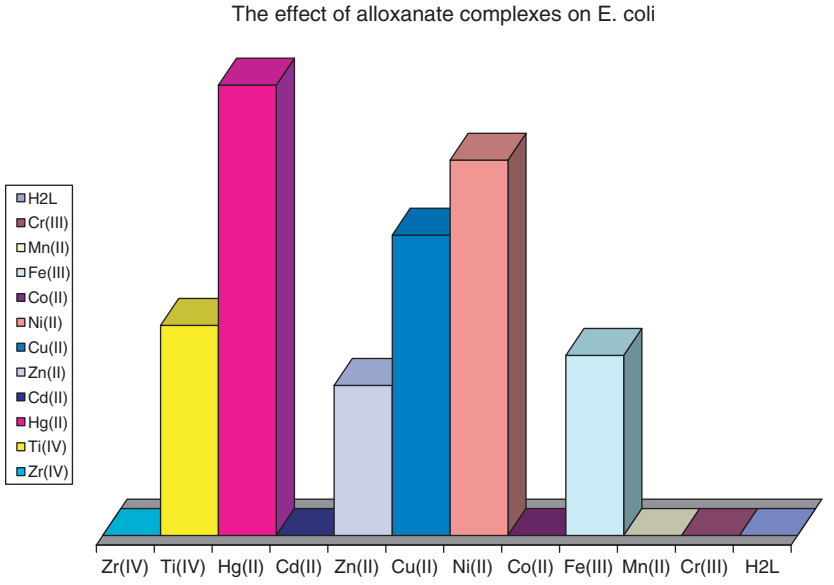

Figure 4. The inhibition zone of alloxan and its metal complexes on *E. coli*.

medium effect on *E. coli*, but lower effect on *Streptococcus pneumonia*. Alloxan and the complexes have also been evaluated for antifungal activity. The minimal inhibitory concentration values listed in table 7 (sample in figure 5) show that all the test compounds have no effect on *Aspergillus Ps* and *Alternaria Ps*, but have high effect on *Penicillium Ps*.

Table 6. Antibacterial activity data of alloxan and complexes.

Compound	*E. coli*	*Streptococcus pneumonia*	*Bacillus subtilis*
H_2L	–	–	+++
1	–	++	–
2	–	–	–
3	++	–	–
4	–	–	+++
5	++++	+++	++
6	++++	+++	++
7	++	++	–
8	–	–	+++
9	++++	++++	+++
10	++	–	+++
11	–	–	+++

(–) no antibacterial activity, (+) Mild activity, (++) Moderate activity, (+++) Marked activity, (++++) Strong activity.

Table 7. Antifungal activity data of alloxan and complexes.

Compound	*Aspergillus Ps.*	*Penicillium Ps.*	*Alternaria Ps.*
H_2L	–	+++	–
1	–	–	–
2	–	++++	–
3	–	+++	–
4	–	++	–
5	–	++++	–
6	–	–	–
7	–	+	–
8	–	++	–
9	–	++	–
10	–	–	–
11	–	++	–

(–) no antibacterial activity, (+) Mild activity, (++) Moderate activity, (+++) Marked activity, (++++) Strong activity.

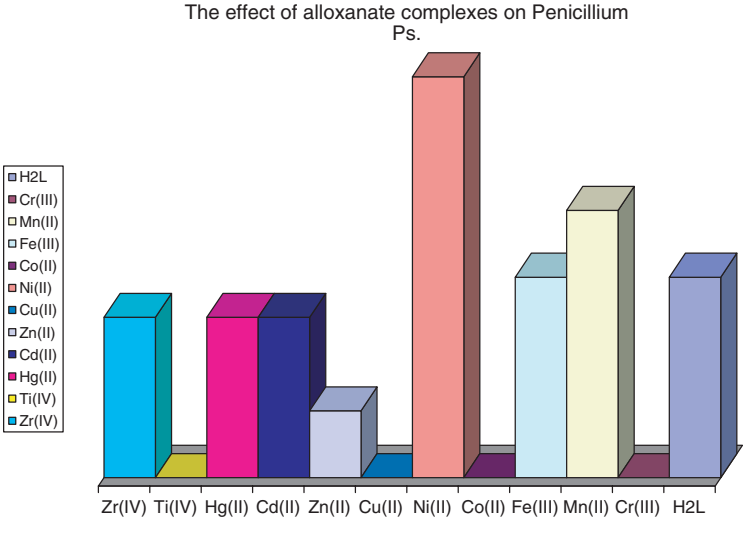

Figure 5. The inhibition zone of alloxan and its metal complexes on *Penicillium Ps.*

References

[1] I. Brugnatelli. *Ann. Chim.*, **8**, 201 (1818).
[2] B.S. Holla, B.S. Rao, B.K. Sarojini, P.M. Akberali. *Eur. J. Med. Chem.*, **39**, 777 (2004).
[3] M. Murata, M. Imada, S. Inoue, S. Kawanishi. *Free Radi. Biol. Med.*, **25**, 586 (1998).
[4] R.E. Heikkila, B. Winston, G. Cohen, H. Barden. *Biochem. Pharmacol.*, **25**, 1085 (1976).
[5] K. Asayama, F. Nyfeler, D. English, S.J. Pilkis, I.M. Burr. *Diabetes*, **33**, 1008 (1984).
[6] K. Jain, J. Logothetopoulos. *Biochim. Biophys. Acta*, **435**, 145 (1976).
[7] H. Yamamoto, Y. Uchigata, H. Okamoto. *Nature*, **294**, 284 (1981).
[8] Y. Uchigata, H. Yamamoto, A. Kawamura, H. Okamoto. *J. Biol. Chem.*, **257**, 6084 (1982).
[9] H. Yamamoto, Y. Uchigata, H. Okamoto. *Biochem. Biophys. Res. Commun.*, **103**, 1014 (1981).
[10] J.T. Bojarski, J.L. Mokrosz, M.N. Paluchowska. *Adv. Heterocycl. Chem.*, **38**, 229 (1985).
[11] D.H.R. Barton, W.D. Ollis (Eds). *Comprehensive Organic Chemistry*, Pergamon, Oxford (1979).
[12] W.E. Lange, W.O. Foyc. *J. Am. Pharm. Ass.*, **45**, 699 (1956).
[13] Yu. Kharitonov, L.N. Ambroladze. *Koord. Khim.*, **9**, 424 (1983).
[14] M.C. Saxena, A.K. Bhattacharya. *Z. Anorg. Allg. Chem.*, **315**, 114 (1962).
[15] G. Deniges. *Bull. Soc. Pharm. Bordeauk*, **3**, 161 (1991).
[16] G. Deniges. *J. Pharm. Chim.*, **11**, 530 (1991).
[17] R.A. Resnik, H. Cecil. *Archives Biochem. Biophys.*, **61**, 179 (1956).
[18] A. Morel, F. Arloing, A. Josserand. *J. Anal. Chem.*, **52**, 674 (1949).
[19] O.V. Kovalchukova, R.K. Gridasova, B.E. Zaitsev. *Zh. Neorg. Khim.*, **26**, 985 (1981).
[20] M.I. Leon Palomino, R.K. Gridasova, B.E. Zaitsev, O.V. Kovalchukova. *Zh. Neorg. Khim.*, **32**, 2583 (1981).
[21] O.V. Kovalchukova, A.K. Molodkin, R.K. Gridasova. *Zh. Neorg. Khim.*, **28**, 1067 (1983).
[22] L.S. Shebaldina, O.V. Kovalchukova, S.B. Strashnova, B.E. Zaitsev, T.M. Ivanova. *Russ. J. Coord. Chem.*, **30**, 38 (2004).
[23] R. Gupta, R.K. Saxena, P. Chatarvedi, J.S. Virdi. *J. Appl. Bacteriol.*, **78**, 378 (1995).
[24] A. von Zelewsky. *Inorg. Chem.*, **20**, 4449 (1981).
[25] C. Daul, E. Deiss, J.N. Gex, D. Perret, D. Schaller, A. Von Zelewsky. *J. Am. Chem. Soc.*, **105**, 7556 (1983).
[26] R. Kakkar, B. Ksarma, V. Katoch. *Proc. Indian Acad. Sci. (Chem. Sci.)*, **113**, 297 (2001).
[27] D. Mootz, G.A. Jeffrey. *Acta Crystallogr.*, **19**, 717 (1965).
[28] C. Singh. *Acta Crystallogr.*, **19**, 759 (1965).
[29] O.V. Kovalchukova, R.K. Gridasova, A.K. Molodkin, N.I. Gavrilova. *Deposited Doc.*, **0**, 95 (1982).
[30] L. Palomino, M. Yvette, R.K. Gridasova, B.E. Zaitsev, O.V. Kovalchukova. *Zhurnal Neorganicheskoi Khimii*, **32**, 2583 (1987).
[31] M.S. Refat. *J. Mol. Struct.* (2007), In press.
[32] K. Nakamato, P.J. Mc Carthy. *Spectroscopy and Structure of Metal Chelate Compounds*, p. 278, John Wiley, New York (1968).
[33] R.H. Holm, F.A. Cotton. *J. Am. Chem. Soc.*, **80**, 5658 (1958).
[34] F.A. Cotton, C.W. Wilkinson. *Advanced Inorganic Chemistry*, 3rd Edn, Interscience Publisher, New York (1972).
[35] B.D. Cullity. *Elements of X-ray Diffraction*, 2nd Edn, Addison-Wesley Inc., New York (1993).
[36] E.S. Freeman, B. Carroll. *J. Phys. Chem.*, **62**, 394 (1958).
[37] J. Sestak, V. Satava, W.W. Wendlandt. *Thermochim. Acta*, **7**, 333 (1973).
[38] A.W. Coats, J.P. Redfern. *Nature*, **201**, 68 (1964).
[39] T. Ozawa. *Bull. Chem. Soc. Jpn.*, **38**, 1881 (1965).
[40] W.W. Wendlandt. *Thermal Methods of Analysis*, Wiley, New York (1974).
[41] H.W. Horowitz, G. Metzger. *Anal. Chem.*, **35**, 1464 (1963).
[42] J.H. Flynn, L.A. Wall. *Polym. Lett.*, **4**, 323 (1966).
[43] P. Kofstad. *Nature*, **179**, 1362 (1957).
[44] J.H.F. Flynn, L.A. Wall. *J. Res. Natl. Bur. Stand.*, **70A**, 487 (1996).